MAGED2 controls vasopressin-induced aquaporin-2 expression in collecting duct cells

Reusch B., Bartram M.P., Dafinger C., Palacio-Escat N., Wenzel A., Fenton R.A., Saez-Rodriguez J., Schermer B., Benzing T., Altmüller J., Beck B.B., Rinschen M.M.

This is the final version of the accepted manuscript. The original article has been published in final edited form in:

Journal of Proteomics
2022 FEB 10 ; 252: 104424
2021 NOV 12 (first published online: final publication)
doi: 10.1016/j.jprot.2021.104424

Publisher: Elsevier

MAGED2 controls vasopressin-induced aquaporin-2 expression in collecting duct cells

Björn Reusch[1,2,11], Malte P. Bartram[2,3,11], Claudia Dafinger[2,3,4], Nicolàs Palacio-Escat[5,6], Andrea Wenzel[1,2], Robert A. Fenton[7], Julio Saez-Rodriguez[5,6,8], Bernhard Schermer[2,3,4], Thomas Benzing[2,3,4], Janine Altmüller[2,9], Bodo B. Beck[1,2,11*], Markus M. Rinschen[2,3,7,10,11*]

[1]Institute of Human Genetics, Faculty of Medicine and University Hospital Cologne, University of Cologne, 50931 Cologne, Germany
[2]Center for Molecular Medicine, Faculty of Medicine and University Hospital Cologne, University of Cologne, 50931 Cologne, Germany
[3]Department II of Internal Medicine, Faculty of Medicine and University Hospital Cologne, University of Cologne, 50937 Cologne, Germany
[4]CECAD, Faculty of Medicine and University Hospital Cologne, University of Cologne, 50931 Cologne, Germany
[5]Joint Research Centre for Computational Biomedicine (JRC-COMBINE), Faculty of Medicine, RWTH Aachen University, 52074 Aachen, Germany
[6]Institute of Computational Biomedicine, Bioquant, Faculty of Medicine, Heidelberg University, 69120 Heidelberg, Germany
[7]Department of Biomedicine, Aarhus University, 8000 Aarhus, Denmark
[8]European Molecular Biology Laboratory, European Bioinformatics Institute, Cambridge CB10 1SD, United Kingdom
[9]Cologne Center for Genomics, University of Cologne, 50931 Cologne, Germany
[10]III Department of Medicine, University Medical Center Hamburg-Eppendorf, 20246 Hamburg, Germany.
[11]These authors contributed equally to this work

[*]e-mail: bodo.beck@uk-koeln.de; rinschen@biomed.au.dk

ABSTRACT

Mutations in the Melanoma-Associated Antigen D2 (*MAGED2*) cause antenatal Bartter syndrome type 5 (BARTS5). This rare disease is characterized by perinatal loss of urinary concentration capability and large urine volumes. The underlying molecular mechanisms of this disease are largely unclear. Here, we study the effect of MAGED2 knockdown on kidney cell cultures using proteomic and phosphoproteomic analyses. In HEK293T cells, MAGED2 knockdown induces prominent changes in protein phosphorylation rather than changes in protein abundance. MAGED2 is expressed in mouse embryonic kidneys and its expression declines during development. MAGED2 interacts with G-protein alpha subunit (GNAS), suggesting a role in G-protein coupled receptors (GPCR) signalling. In kidney collecting duct cell lines, *Maged2* knockdown subtly modulated vasopressin type 2 receptor (V2R)-induced cAMP-generation kinetics, rewired phosphorylation-dependent signalling, and phosphorylation of CREB. *Maged2* knockdown resulted in a large increase in aquaporin-2 abundance during long-term V2R activation. The increase in aquaporin-2 protein was mediated transcriptionally. Taken together, we link MAGED2 function to cellular signalling as a desensitizer of V2R-induced aquaporin-2 expression.

1. Introduction

"Bartter syndrome" is a medical term for a group of rare inherited kidney disorders. Patients with Bartter syndrome show a loss of urinary concentration capability due to loss of function of renal transporters or channels in the kidney nephron. This forces them to excrete large volumes of urine every day, posing a potentially life-threatening condition. Commonly observed are salt wasting, electrolyte disturbances, polyuria, hypotension, decreased quality of life, and potentially end stage renal disease. The condition requires life-long symptomatic treatment [1-7]. Mutations in the Melanoma-Associated Antigen D2 (*MAGED2*) cause Bartter syndrome type 5 (BARTS5) (OMIM#300971) [8]. Compared to other forms of Bartter syndrome, the BARTS5 type presents around birth, and shows severe polyhydramnios *in utero* with an increased risk for premature delivery and perinatal mortality. Salt loss and large urinary volumes can persist into the postnatal period for months [8, 9]. In contrast to all other forms of Bartter syndrome, BARTS5 is inherited X-linked and resolves completely [8]. In a recent cohort, 10% of antenatal Bartter syndromes had pathogenic MAGED2 mutations [9]. In addition, *MAGED2* is ubiquitously expressed and has been linked to development [10, 11].

It is unclear how MAGED2 participates in the regulation of kidney transport functions. In our initial studies, kidney tubules of the sodium transporters NKCC2 and NCC were decreased in available kidney sections from one diseased foetus [8]. Moreover, knockdown of *MAGED2* in HEK293T cells overexpressing the co-transporters led to impaired maturation (glycosylation) of NKCC2 and NCC *in vitro* [8]. However, the precise molecular mechanisms underlying *MAGED2* associated Bartter syndrome could not be explained so far. Previously, we also showed via interactome analyses that wild-type (WT), but not the recurrent missense variant R446C, interacts with the stimulatory G-protein alpha subunit (GNAS) [8]. GNAS associates with G-protein coupled receptors and mediates signals from the cell surface to intracellular effectors via cAMP-dependent signalling pathways [12]. Activation of a Gs-α-coupled transmembrane receptor activates downstream effectors such as adenylyl cyclase, which in turn catalyses the transformation of ATP to the second messenger cAMP [13]. Increasing cAMP levels [14] and the activation of specific cAMP-dependent pathways[15, 16] are crucial for proper kidney development and function. In addition to these finding, Maged2 physically interacts with p53 and regulates cell cycle [17]. MAGED2 has also been recognized as a diagnostic marker in cancer [18, 19].

The aim of this study was to further analyse the signalling of MAGED2 in its ability to modulate G-protein coupled receptor signalling in a cell culture model of the distal nephron. As a model system, we chose HEK293T cells and mouse collecting duct cells (mpkCCD), a cell line derived from the distal tubule that responds to vasopressin and aldosterone without further manipulation [20, 21]. We chose this cell line because a thick-ascending limb cell-line with endogenous NKCC2 and NCC protein expression is currently not available [22, 23].

2. Methods

2.1 Cell culture

HEK293T cells were maintained in Dulbecco's modified Eagle's medium (DMEM) containing 10% FCS in an incubator at 37°C with 5% CO_2.
Mouse collecting duct principal (mpkCCD) cells were maintained in a 1:1 mixture of Dulbecco's modified Eagle's medium and Ham's F-12 Nutrient Mixture (DMEM-F12) containing 5 µg/ml insulin, 50 nM dexamethasone, 1 nM triiodothyronine, 10 ng/ml epidermal growth factor, 60 nM sodium selenite, 5 µg/ml transferrin and 2% bovine serum in an incubator at 37°C with 5% CO_2 [21].

For experimental procedures the cells were seeded on permeable filters (Transwell permeable supports, 0.4 µm pore size, 24 mm diameter, Corning Costar) until confluency and polarization. Vasopressin treatment schemes were according to previously published studies [20, 24]. Long-term treatment was performed with 1 nm of the stable and V2-specific agonist 1-deamino-8-D-arginine vasopressin (dDAVP) for 72 hours with daily changes of the medium for induction of aquaporin 2 (AQP2) expression. Short-term treatments also included an initial long-term treatment of the cells with 1 nm dDAVP over a period of 72 hours with a subsequent dDAVP withdrawal phase of 6 hours followed by short-term incubation with 1 nm dDAVP for 30 minutes. dDAVP treatments were performed in the absence of supplements and growth factors.

2.2 siRNA and transfection

Endogenous MAGED2 expression was knocked down in HEK293T cells with a mixture of MAGED2 siRNAs (1: GGACGAAGCUGAUAUCGGA, 2: GCUAAAGACCAGACGAAGA, 3: AGGCGAUGGAAGCGGAUUU, 4: GAAAAGGACAGUAGCUCGA; Dharmacon). As a control, scrambled control siRNA was used (UGGUUUACAUGUCGACUAA, Dharmacon). For this purpose, 30 pmol of either siRNA were transfected in HEK293T cells with Lipofectamine 2000 according to the manual and the cells were incubated at 37°C for 48 hours. The cell pellets were then used for the proteome and phospho-proteome analyses.

2.3 shRNA and generation of stable cell lines

The shERWOOD algorithm was utilized (http://sherwood.cshl.edu:8080/sherwood) to predict efficient shRNA sequences[25]. The hairpin sequences targeting MAGED2 (mMageD2_shERWOOD-no3: GCTGTTGACAGTGAGCGAAACTGGGACGAAGCTG ATATATAGTGAAGCCACAGATGTATATATCAGCTTCGTCCCAGTTGTGCCTACTG CCTCGGA; mMageD2_shERWOOD-no4: TGCTGTTGACAGTGAGCGAACCTACCA CACAGCTGAGTGATAGTGAAGCCACAGATGTATCACTCAGCTGTGTGGTAGGTG TGCCTACTGCCTCGGA) and the control hairpin sequences targeting the renilla luciferase (TGCTGTTGACAGTGAGCGCAGGAATTATAATGCTTATTGCTGTTGACA GTGAGCGCAGGAATTATAATGCTTATCTATAGTGAAGCCACAGATGTATAGATAA GCATTATAATTCCTATGCCTACTGCCTCGGA) were amplified by PCR and sub-cloned into a modified PiggyBac PB-CMV-GreenPuro-H1-MCS shRNA Expression vector (Systembio, Cat. No. PBSI50A-1). All constructs were verified by sequencing.

To generate stable cell lines that express the hairpins mpkCCD cells were

transfected with the hairpin constructs and the PiggyBac Transposase vector (pCMV hyPase). Selection with 2 µg/ml puromycin was started 48 hours after transfection.
Knockdown efficiency was determined by mMageD2 qPCR (mMAGED2 fp: 5´-GAGAGGGACTGAGAGGAGCA; mMAGED2 rp: 5´- CCACTCTCGCTTGTGTCAGA) using mACTB (fp: 5` - aag agc tat gag ctg cct ga; rp: 5` - tac gga tgt caa cgt cac ac) and mHPRT1(fp: 5´ - gct gac ctg gat tac at; rp: 5´- ttg ggg ctg tac tgc tta ac) as housekeeping genes as well as Western blot analysis.

2.4 Mouse embryonic kidneys

All animal procedures were performed in accordance with European (EU directive 86/609/EEC), national (TierSchG), and institutional guidelines and were approved by local governmental authorities (LANUV NRW, AZ 84–02.04.2013.A152). All experiments were performed in compliance with the ARRIVE guidelines[26]. The mice were housed according to the standardized specific pathogen-free conditions in the animal facility of the University of Cologne. Newborn and embryonic mice were sacrificed by decapitation and pregnant mice were sacrificed by cervical dislocation after removing all embryos under deep narcosis. Tissue was processed by snap freezing in tissue embedding compound (Tissue-Tek O.C.T., Sakura).
Genotyping for sex determination was performed by amplifying the Y-chromosome-specific SRY gene using the primers SRY-fp (5'-tgg gac tgg tga caa ttg tc-3') and SRY-rp (5'-gag tac agg tgt gca gct ct-3'). IL3 was amplified in parallel as internal PCR control using the primers IL3-fp (5'-ggg act cca agc ttc aat ca-3') and IL3-rp (5'- tgg agg aag aaa agc aa-3').

2.5 Antibodies

The following primary antibodies were used for the Western Blot experiments in the indicated dilution: anti-HA (Roche; rat; 11867423001; 1:2,000), anti-FLAG (Sigma-Aldrich; mouse; F1804; 1:20,000), anti-MAGED2 (a gift by Olivier de Backer; rabbit; 1:1,000), anti-AQP2 (Alomone; rabbit; AQP2-002; 1:2,000), anti-pCREB (Ser133) (Cell Signaling, rabbit; 87G3; 1:1,000), anti-CREB1 (Santa Cruz; mouse; Sc-377154; 1:1,000), anti-p-p44/42 MAPK (Thr202, Tyr204/Thr185, Tyr 187) (Cell Signaling; rabbit; D13.14.4E; 1:1,000), anti-p44/42 MAPK (Cell Signaling; rabbit; 9102; 1:1,000) and pAQP2 (Ser256) (PhosphoSolutions; rabbit; 1697; 1:1,000). The following secondary antibodies were used in the indicated dilutions: HRP-coupled goat anti mouse (Santa Cruz; Sc-2005; 1:10,000), HRP-coupled goat anti-rabbit (Santa Cruz; Sc-2004; 1:10,000) and HRP-coupled goat anti-rat (Santa Cruz; Sc-2006; 1:10,000).

2.6 Immunoblotting

HEK293T and mpkCCD cells grown on permeable filters were lysed with a buffer containing 0.25% or 4% SDS, respectively. Subsequently, the protein lysates were mechanically shredded by use of Qiagen shredder columns and denaturated by incubation at 96°C for 10 minutes in 4x Laemmli sample buffer from Bio-Rad containing 10% mercaptoethanol. 10 µg of the protein samples were then separated on a 12% SDS-PAGE gel using the Mini-PROTEAN Tetra cell system from Bio-Rad. Transfer of the proteins from the gel to a nitrocellulose membrane occurred with the Trans-Blot Turbo Transfer system from Bio-Rad. The blots were then blocked with 5% BSA or

milk in Tris-buffered saline with Tween-20 (TBST) for one hour at room-temperature. After the blocking the membranes were incubated with the first antibody in blocking buffer at 4°C overnight. After three washing steps with TBST, treatment with the peroxidase-conjugated secondary antibody followed which occurred in TBST for 45 minutes at room-temperature. The peroxidase reaction was induced by using the Clarity Western ECL Substrate and the blots were then developed in the chemidoc XRS from Bio-Rad.

Densitometric quantification was determined with Image Lab from Bio-Rad. Statistical analysis was performed with Excel from Microsoft and Prism 7.03 from GraphPad using a Dunnetts test with Tukeys post-test or t-test as indicated in the figure legends.

2.7 cAMP assay

Direct cAMP concentrations in short-term treated mpkCCD cells were measured with a commercially available ELISA kit (R&D Systems, KGE002B) according to the manufacturer's instructions. In brief, one confluent well of a 6 well transwell plate was diluted 1:10 and lysate (in the lysate buffer provided by the manufacturer) was used as an input for the analysis. The assay was performed exactly as indicated by the manufacturer's instructions. The data were acquired using a PerkinElmer plate reader.

2.9 qPCR analyses

Total RNA was isolated from long-term treated mpkCCD cells by using the RNeasy Mini Kit from Qiagen according to the manual. The RNA was then used as template for quantitative PCR (qPCR) analysis with the Power SYBR Green RNA-to-CT 1-Step Kit to analyse changes of the expression in long-term treated mpkCCD cells. The quantification was performed by using the ΔΔCt method with a normalization of the resulting cycle threshold (Ct) values on the basis of actin mRNA. Fold changes were indicated as changes of mRNA expression levels in relation to the vehicle treated control.

2.10 qPCR primers

The following primer pairs were used for the qPCR analyses: Maged2 (fp: 5´-GAGAGGGACTGAGAGGAGCA, rp: 5´- CCACTCTCGCTTGTGTCAGA), Actb (fp: 5` - AAG AGC TAG GAG CTG CCT GA, rp: 5` - TAC GGA TGT CAA CGT CAC AC), mHPRT1 (fp: 5´ - GCT GAC CTG GAT TAC AT, rp: 5´- TTG GGG CTG TAC TGC TTA AC), Slc12a1 /Nkcc2 (fp: 5´- TGG CGT GGT CAT AGT CAG AA, rp: 5´- GCC AAT CTC TCC TGT TCC AG), Slc12a3/Ncc (fp1: 5´- GCT TCT TTG GCA TGT TCT CC, rp1: 5´- TCC AGA AAA TGG CCA TGA GT), Aqp2 (fp: 5´- CCT CCA TGA GAT TAC CCC, rp: 5´- GGA AGA GCT CCA CAG TCA CC), Actb (fp2: 5' - CTG GCT CCT AGC ACC ATG AA, rp2: 5' - AGC TCA GTA ACA GTC CGC CTA), V2R (fp: 5' - GTG TCT ACC ACG TCT GTG CC, rp: 5' - CAA GGC CAC AGC CAC AAA AA) and EnAC (fp: 5' – GCA GGC CAC CAA CAT CTT CT, rp: 5' – TAG GCG TGA AGT TCC GAT GAC).

2.11 Sample preparation for proteomics and phosphoproteomics

Sample preparation for phosphoproteomics was performed as previously described [24, 27]. In brief, mpkCCD or HEK293T cells were lysed using 8M urea and 50mM ammonium bicarbonate. Protease and phosphatase inhibitor cocktail (1x, Pierce) had been previously added in the lysis buffer. Proteins were reduced using 10mM DTT for 1h at room temperature and alkylated using Iodoacetamide, 40mM for 1h in the dark. Then, urea was diluted to less than 2M, and 1:100 trypsin was added to the mix and proteins were digested for 16h on a shaker. After desalting, 800ug of digested peptides were subjected to phosphopeptide enrichment using IMAC Fe-NTA columns (Thermo fisher). Eluted peptides were cleaned up using stage tips [28]. Sample preparation for proteomics was performed using an in-solution digestion as described above, followed by stage tips. The replicates are biological replicates. Peptides were separated using a reverse phase separation using a nLC followed by analysis on a Q Exactive plus mass spectrometer essentially as previously described [29]. One technical run per sample was performed. Overall, 5 replicates were performed for HEK293T cells and n=3 for mpkCCD cells. The raw data of the study are available as PRIDE/ProteomExchange ID PXD005801, PXD008062 and PXD008059 [30, 31].

2.12 Proteomics data processing

Dataset was processed using MaxQuant v 1.5.1.3[32] and were subsequently analysed using Perseus v.1.5.5.3 [33]. The Label free quantification (LFQ) option in MaxQuant was enabled. LFQ Data were log2 transformed, and both contaminants and reverse proteins were filtered out. Effect sizes (log2 dDAVP/control) were plotted against each other in both cell lines. Analysis similar to significance in microarrays by Tusher et al. was performed to determine significantly changed proteins using the given thresholds [34]. Motif analyses were performed using icelogo [35].

2.13 Phosphorylation network analysis

Based on the effect size data, the differential phosphorylation (dDAVP vs. control) was computed by fitting a linear model for each site for both conditions. The corresponding t- and p-values were obtained by using the empirical Bayes method with R's 'limma' package v3.34.9 [36]. Phosphorylation network analysis was performed with the PHONEMeS tool using the obtained log2 fold-changes (FC) from the MAGED2 knockdown and control cell lines against a kinase-substrate network obtained from OmniPath (November 2017)[37, 38]. In order to study the downstream phosphorylation signalling of V2R upon stimulation, PKA was regarded as the most direct effector kinase (GPCR -> AC -> cAMP -> PKA) and source of the perturbation for the analysis. The effect size of a given phosphorylation site was considered significant if its value was at least 1.5 times higher or lower than the median FC and p-value below 0.2. The resulting networks were plotted using Cytoscape v3.5.1. The scripts for the analysis can be found in the following repository: https://github.com/saezlab/MAGED2_phospho.

3. Results

3.1 MAGED2 is expressed in the mouse kidney in early embryonic stages

To investigate the role of MAGED2 in the developing kidney we analysed its expression in mouse embryonic tissue during development. mRNA expression analysis showed high *Maged2* mRNA levels at stage E14.5 and a decrease at stage E18.5 and at birth (Fig. 1A). The mRNA level of *Maged2* was not significantly different between male and female mice (Fig. S1) despite its genomic localization on the X chromosome. Concurrent with decreased *Maged2* expression, the relative expression of the essential renal transport proteins *Slc12a3* (NCC), *Slc12a1* (NKCC2) and *Aqp2* increased during renal development (Fig. 1B).

3.2 MAGED2 is a putative regulator of G-protein coupled receptor signalling

MAGED2 is endogenously expressed in HEK293T cells (Fig. 2A). To investigate functions of MAGED2 in HEK293T cells, we performed proteomic analysis of HEK293T cells with and without *MAGED2* knockdown using siRNA. Western Blot and initial proteomic analysis confirmed successful knockdown of *MAGED2* after 48h with a residual MAGED2 expression of approximately 11.6% (SD=2.4%) in the siRNA treated sample (Fig. 2A and 2B). Surprisingly, statistical analyses revealed no other proteins being differentially expressed in the *MAGED2* knockdown cells in comparison to the controls. To investigate effects of the *MAGED2* knockdown that are mediated on a posttranscriptional level, phosphoproteomic analysis was performed with the same cells (Fig. 2C). In contrast to the proteome data, these results showed strong alterations of the phosphorylation status within the cells. In particular, a perturbation of basophilic kinase associated phosphorylation motifs was observed (Fig. 2D and 2E). Phosphorylation changes induced by the *MAGED2* knockdown were larger than proteome alterations (Fig. 2F). These findings are consistent with a role of MAGED2 on the posttranslational signalling landscape. This suggests that MAGED2 is a modulator of signalling processes rather than a direct regulator of protein expression.

Previous studies from our and other groups showed an association of MAGED2 with the small G-protein Gsalpha (Gene symbol: GNAS) and therefore a potential role in G-protein coupled receptor signalling [8, 39]. We mined dynamic G-protein coupled receptor interactome datasets to corroborate this hypothesis. Paek et al. [40] used ascorbate peroxidase-catalysed proximity labelling (APEX) to trail GPCR signalling in living cells: in this dataset, MAGED2 was found as a protein associated with the angiotensin II type 1 receptor (Fig. 2G) as well as the β2 adrenergic receptor (Data not shown). These studies suggest a modulating effect of MAGED2 on GPCR signalling.

3.3 MAGED2 modulates short-term V2R dependent signalling in mpkCCD cells

The interaction of MAGED2 with GNAS suggests a role of MAGED2 in cAMP-dependent signalling pathways. For these reasons, we chose the mouse cortical duct cell line mpkCCD for subsequent experiments. This kidney cell line is sensitive to vasopressin (dDAVP) exposure with physiological concentrations. The stable

vasopressin-analogon dDAVP activates the GPCR AVPR2, which leads to an increase in intracellular cAMP. This results in protein kinase A dependent phosphorylation and trafficking of AQP2 (short-term exposure) and increased transcription/translation of AQP2 (long-term exposure)[20]. Each short-term exposure is preceded by a long-term exposure followed by a dDAVP starvation in order to accomplish a sufficient amount of the proteins involved in the AQP2 pathway.

To investigate the role of MAGED2 in the cAMP-dependent pathway, we generated cell lines with stable knockdown of *Maged2* in mpkCCD cells (Fig. 3A and 3B). To measure changes of cAMP levels due to *Maged2* knockdown, we performed cAMP-assays with these cells. After dDAVP treatment cAMP levels were measured after 2 minutes, 30 minutes and 120 minutes. There was an increase of cAMP after 2 minutes and a subsequent decrease until 120 minutes in the control cells, and this curve was steeper after *Maged2* knockdown. There was a higher increase in cAMP levels after 2 minutes followed by a decrease with significantly lower cAMP levels after 30 minutes in the *Maged2* knockdown cells. After 120 minutes the cAMP levels in all samples decreased to a similar level (Fig. 3C).

A target of increased cAMP levels is the protein cAMP response element-binding protein (CREB). This transcription factor is activated upon phosphorylation by several putative kinases including protein kinase A (PKA) and protein kinase C (PKC)[41]. We performed short-term treatment of mpkCCD cells with dDAVP for 30 minutes. While there was an increase of pCREB in the vehicle treated control cells with functional MAGED2, this increase was significantly less (or partly reversed) in the *Maged2* knockdown cells (Fig. 3D). Previous studies also showed that vasopressin treatment decreases phosphorylated ERK activity in the same cell line[24]. Consistent with these findings, pERK levels decreased upon dDAVP treatment comparably (Fig. 3E), indicating a complex role of MAGED2 in cAMP dependent signalling.

To further analyse the mechanism, we used phosphoproteomic analysis using a label-free approach. In total, 12456 phosphorylation sites were identified after filtering. Quantitative statistical analyses, including correction for multiple testing were performed. First, we analysed the regulated phosphorylation motifs of vasopressin-dependent signalling in our *Maged2* knockdown cells vs controls. No overt switch in vasopressin-induced phosphorylation patterns was observed (Figure 3F,G). After annotation of phosphorylation sites that are linked to function, the data revealed subtle alterations in the *Maged2* vs. control samples (black dots), but none of them reached significance. The overall fraction of basophilic sites was reduced in dDAVP treated cells with *Maged2* depletion (Fig. 3F, G and H). In total, overlap between statistical induced phosphorylation sites in Maged2 and control was less than 10%, suggesting complex rewiring of signalling.

To further model this, we performed additional computational analyses using the PHONEMeS tool (PHOsphoproteomic NEtworks for Mass Spectrometry) [38]. This algorithm investigates changes in phosphorylation upon perturbation against a background kinase-substrate network, allowing to annotate and model signalling patterns. These data suggested potential rewiring of various non-canonical GPCR-associated pathways (Fig. S2). Comparison of the results between control and MAGED2 knockdown cells showed some alterations in several pathways including AKT/mTOR, ERK, JNK and CDK-related pathways. Therefore, we conclude that modulation of the downstream phosphoproteome of short-term vasopressin signalling was observable, yet with only subtle inhibition of cAMP response.

3.4 MAGED2 modulates long-term V2R dependent signalling in mpkCCD cells

While short-term dDAVP treatment of mpkCCD cells leads to cAMP-dependent phosphorylation processes of AQP2, long-term dDAVP treatment presumably acts on a transcriptional program dependent on protein kinase A[42]. To analyse the consequences of *Maged2* knockdown in this context, we treated mpkCCD cells with dDAVP over a time span of 72 hours. Proteome analysis revealed an enrichment of the proteins MED14 and AQP2 in both the *Maged2* knockdown and control cells after dDAVP treatment. However, the vasopressin induced abundance of both proteins was significantly higher in the knockdown cells than in the control cells (Fig. 4A). Analysis of mRNA expression confirmed that this finding was due to changes on the transcriptional level (Fig. 4B) like an increased *Aqp2* transcription or a decreased *Aqp2* mRNA turnover. Also, Western Blot analyses of long-term treated mpkCCD cells with dDAVP showed a significant higher increase of AQP2 protein in the *Maged2* knockdown cells compared with the control cells confirming this finding (Fig. 4C). As a result of this elevated total AQP2 protein amount, we could also observe an increase of phosphorylated AQP2 in long-term treated mpkCCD cells in a subsequent short-term stimulation (Fig. S3). Maged2-dependent changes of *Avpr2* (V2R) and *Scnn1b* (β-subunit of EnAC) mRNA expression after dDAVP treatment were not observed (Fig. S4 and S5).

4. Discussion

Rare genetic diseases offer a unique window to understand human physiology and tackle disease. Bartter syndrome leads to huge urinary volumes due to lack of urine concentration. The widely-used diuretic drugs furosemide and thiazide target the gene products mutated in some forms of Bartter syndrome, viz. Slc12a1 (NKCC2), and Slc12a3 (NCC). Given this clinical relevance, it is even more important to understand the molecular mechanisms of a recently emerged form of Bartter syndrome, Bartter syndrome Type 5. MAGED2 mutations form a novel disease entity, Bartter syndrome type 5, BARTS5 (OMIM#300971), as confirmed by other groups [9, 43]. Despite its recent discovery, they account for a substantial proportion of unresolved cases and approximately constitute 10% of all Bartter syndrome cases [9]. MAGED2 is not a transporter or channel, and little is known about the physiological role of MAGED2 in kidney cells. Here, we followed the new hypothesis that MAGED2 has a signalling role on proteome level.

In this study, we performed first proteome-based exploratory experiments to understand MAGED2 function. Exploratory proteomics studies in HEK293T suggested that MAGED2 is capable of altering phosphorylation patterns. More detailed proteomic and phosphoproteomic studies were then performed in mpkCCD. These cells offer several advantages: First, it is a polarized collecting duct cell line that expresses MAGED2 endogenously [44]. Second, the mpkCCD cells are a well-established model for vasopressin signalling [45] and the cell line responds to physiological concentrations of dDAVP. These cells exhibit a cAMP-coupled short-term response as well as a cAMP-independent long-term response [20, 24] with subsequent aquaporin-2 expression. The cells do not increase phosphorylation of the site Aquaporin-2 site Ser256 in response to vasopressin [20]. To our knowledge, there are no other cell lines available with endogenous expression of a GNAS-coupled GPCR, or other transporters involved in solute homeostasis.

We observed that *Maged2* knockdown affects both short-term and long-term vasopressin-dependent signalling. Short-term treatment of the mpkCCD cells with dDAVP revealed that *Maged2* knockdown affected cAMP level kinetics as well as the amount of the phosphorylated target protein CREB. This suggests an altered AVPR2 response to dDAVP treatment. Our main finding, however, was a strong increase in *Aqp2* mRNA levels and protein expression in the MAGED2 depleted cell lines in response to long-term dDAVP treatment, while the mRNA expression of the β-subunit of ENaC as another vasopressin-controlled channel protein, did not increase. Also, we could not observe an altered increase of *Avpr2* (V2R) expression in the *Maged2* depleted cells, which as GPCR influences intracellular cAMP levels. One explanation for this could be the increased expression of MED14 as observed on protein level. This protein depicts a subunit of the mediator complex that plays an important role as mediator of transcription factors and RNA polymerase II [46]. It is also regulated by vasopressin treatment and translocates in the nucleus [46, 47]. Therefore, it could activate transcriptional processes that increase the vasopressin-induced AQP2 levels in *Maged2* knockdown mpkCCD cells (Fig. 4B). This is consistent with the finding that each mediator subunit protein regulates the expression of a definite subset of genes and not the entire process of transcription [46]. In addition, MED14 is part of a known

vasopressin-response complex in this cell culture model[47], and AQP2 is one of the most strongly induced transcripts and proteins in this cell culture model.

The dataset presented here can also be used to generate novel hypotheses regarding the effect of MAGED2 on cell physiology, especially in the context of AQP2 regulation. Several transcription factors have been linked to the expression of AQP2, including Elf3 (Ets), Jun, Gata, NFAT transcription factors and others [20, 48-50]. It will be of importance to investigate whether MAGED2 modulates its activity, especially since some of these transcription factors are also involved in the control of other salt transporters[51]. The present literature already demonstrates functional MAGED2 interactions with some stress response transcriptional genes. In human cancer cells MAGED2 interacts with the transcriptional factor tumour suppressor protein p53 and impairs its transcriptional ability [17]. MAGED2 knockdown also increased the transcription of p53 itself [52]. It also negatively regulates the expression of tumour necrosis factor-related apoptosis-inducing ligand (TRAIL) death receptor 2 (TRAIL-R2) and saves cancer cells from TRAIL-induced apoptosis [46].

The phenotype of an increased AQP2 abundance in *Maged2* depletion observed here *in vitro* would lead to an increased reabsorption of water resulting in hyponatremia *in vivo*. Hyponatremia has been described in the patients in the initial cohort [8, 9], and is anecdotally observed in patients with Bartter syndrome [53]. However, fluid resuscitation [54] in clinical practice can potentially contribute to this phenotype [8, 9, 20]. To answer how loss of MAGED2 during kidney development induces alterations to physiological processes or if AQP2 abundance plays a protective role in the course of the disease and contributes to its transient character, will further have to be studied *in vivo* or in organoids. In addition, we observed some perturbations of b-Arrestin mediated signalling pathways such as AKT (Fig. S2), but we were not able to systematically investigate the role of MAGED2 in b-Arrestin mediated signalling. B-Arrestin modulates a large fraction of GPCR dependent processes [55]. For instance, GNAS and b-Arrestin complexes mediate long-term sustained GPCR signalling [56]. It will be of interest to further dissect the interplay between these signalling relays in the future. We hypothesize that MAGED2 may be an overall desensitizer of outside-in signalling. Consistent with this are the slightly altered cAMP kinetics (Fig. 3C) and, notably, the stronger expression of AQP2. We suggest that this process could also be PKA-independent [57].

5. Conclusions

In conclusion we report that MAGED2 regulates vasopressin-induced protein and phosphorylation patterns in a kidney collecting duct cell line and provide a broad resource for further studying MAGED2 actions in development and disease.

Acknowledgements: The authors thank Olivier de Backer for providing us with the anti-MAGED2 antibody [8]. We thank all members of our groups for helpful discussions and Martyna Brütting and Ruth Herzog for excellent technical assistance.

Funding

This work was supported by the Koeln Fortune Program/Faculty of Medicine grant (KF 245/2014) and the CMMC (B.B.B.). M.P.B. was supported by an intramural grant of the University of Cologne (Gerok program), N.P. by the JRC for Computational Biomedicine which was partially funded by Bayer AG and M.M.R. by the DFG (RI2811/1-1 and RI2811/2-1).

Author contributions

B.R., M.P.B., M.M.R. and B.B.B. contributed equally to this work. B.R. and M.P.B. planned the *in vitro* work, performed experiments, analysed the data and wrote the manuscript; C.D. performed the *in vivo* work and interpreted the data; N.P.E., A.W., R.A.F., J.S.R., B.S, T.B, and J.A. contributed to the advancement of the project; B.B.B. designed and supervised the project, interpreted the data, and wrote the manuscript; M.M.R. designed and supervised the project, interpreted the data, performed experiments and wrote the manuscript. All authors reviewed the manuscript.

Conflict of interest: The authors declare that they have no conflicts of interest with the contents of this article.

Correspondence should be addressed to B.B.B. and M.M.R.

References

[1] D.B. Simon, F.E. Karet, J.M. Hamdan, A. DiPietro, S.A. Sanjad, R.P. Lifton, Bartter's syndrome, hypokalaemic alkalosis with hypercalciuria, is caused by mutations in the Na-K-2Cl cotransporter NKCC2, Nat Genet 13(2) (1996) 183-8.
[2] D.B. Simon, F.E. Karet, J. Rodriguez-Soriano, J.H. Hamdan, A. DiPietro, H. Trachtman, S.A. Sanjad, R.P. Lifton, Genetic heterogeneity of Bartter's syndrome revealed by mutations in the K+ channel, ROMK, Nat Genet 14(2) (1996) 152-6.
[3] D.B. Simon, R.S. Bindra, T.A. Mansfield, C. Nelson-Williams, E. Mendonca, R. Stone, S. Schurman, A. Nayir, H. Alpay, A. Bakkaloglu, J. Rodriguez-Soriano, J.M. Morales, S.A. Sanjad, C.M. Taylor, D. Pilz, A. Brem, H. Trachtman, W. Griswold, G.A. Richard, E. John, R.P. Lifton, Mutations in the chloride channel gene, CLCNKB, cause Bartter's syndrome type III, Nat Genet 17(2) (1997) 171-8.
[4] R. Birkenhager, E. Otto, M.J. Schurmann, M. Vollmer, E.M. Ruf, I. Maier-Lutz, F. Beekmann, A. Fekete, H. Omran, D. Feldmann, D.V. Milford, N. Jeck, M. Konrad, D. Landau, N.V. Knoers, C. Antignac, R. Sudbrak, A. Kispert, F. Hildebrandt, Mutation of BSND causes Bartter syndrome with sensorineural deafness and kidney failure, Nat Genet 29(3) (2001) 310-4.
[5] K.P. Schlingmann, M. Konrad, N. Jeck, P. Waldegger, S.C. Reinalter, M. Holder, H.W. Seyberth, S. Waldegger, Salt wasting and deafness resulting from mutations in two chloride channels, The New England journal of medicine 350(13) (2004) 1314-9.
[6] R. Kleta, D. Bockenhauer, Bartter syndromes and other salt-losing tubulopathies, Nephron Physiol 104(2) (2006) p73-80.
[7] H.W. Seyberth, K.P. Schlingmann, Bartter- and Gitelman-like syndromes: salt-losing tubulopathies with loop or DCT defects, Pediatr Nephrol 26(10) (2011) 1789-802.
[8] K. Laghmani, B.B. Beck, S.S. Yang, E. Seaayfan, A. Wenzel, B. Reusch, H. Vitzthum, D. Priem, S. Demaretz, K. Bergmann, L.K. Duin, H. Gobel, C. Mache, H. Thiele, M.P. Bartram, C. Dombret, J. Altmuller, P. Nurnberg, T. Benzing, E. Levtchenko, H.W. Seyberth, G. Klaus, G. Yigit, S.H. Lin, A. Timmer, T.J. de Koning, S.A. Scherjon, K.P. Schlingmann, M.J. Bertrand, M.M. Rinschen, O. de Backer, M. Konrad, M. Komhoff, Polyhydramnios, Transient Antenatal Bartter's Syndrome, and MAGED2 Mutations, The New England journal of medicine 374(19) (2016) 1853-63.
[9] A. Legrand, C. Treard, I. Roncelin, S. Dreux, A. Bertholet-Thomas, F. Broux, D. Bruno, S. Decramer, G. Deschenes, D. Djeddi, V. Guigonis, N. Jay, T. Khalifeh, B. Llanas, D. Morin, G. Morin, F. Nobili, C. Pietrement, A. Ryckewaert, R. Salomon, I. Vrillon, A. Blanchard, R. Vargas-Poussou, Prevalence of Novel MAGED2 Mutations in Antenatal Bartter Syndrome, Clinical journal of the American Society of Nephrology : CJASN 13(2) (2018) 242-250.
[10] M. Bertrand, I. Huijbers, P. Chomez, O. De Backer, Comparative expression analysis of the MAGED genes during embryogenesis and brain development, Developmental dynamics : an official publication of the American Association of Anatomists 230(2) (2004) 325-34.
[11] J. Chelly, J.L. Mandel, Monogenic causes of X-linked mental retardation, Nat Rev Genet 2(9) (2001) 669-80.
[12] L.S. Weinstein, S. Yu, D.R. Warner, J. Liu, Endocrine manifestations of stimulatory G protein alpha-subunit mutations and the role of genomic imprinting, Endocr Rev 22(5) (2001) 675-705.
[13] S. Turan, M. Bastepe, GNAS Spectrum of Disorders, Curr Osteoporos Rep 13(3) (2015) 146-58.
[14] D. Schlondorff, H. Weber, Cyclic nucleotide metabolism in compensatory renal hypertrophy and neonatal kidney growth, Proc Natl Acad Sci U S A 73(2) (1976) 524-8.
[15] X. Li, H.P. Li, K. Amsler, D. Hyink, P.D. Wilson, C.R. Burrow, PRKX, a phylogenetically and functionally distinct cAMP-dependent protein kinase, activates renal epithelial cell migration and morphogenesis, Proc Natl Acad Sci U S A 99(14) (2002) 9260-5.
[16] B. Neubauer, K. Machura, M. Chen, L.S. Weinstein, M. Oppermann, M.L. Sequeira-Lopez, R.A. Gomez, J. Schnermann, H. Castrop, A. Kurtz, C. Wagner, Development of vascular renin expression in

the kidney critically depends on the cyclic AMP pathway, Am J Physiol Renal Physiol 296(5) (2009) F1006-12.
[17] C. Papageorgio, R. Brachmann, J. Zeng, R. Culverhouse, W. Zhang, H. McLeod, MAGED2: a novel p53-dissociator, International journal of oncology 31(5) (2007) 1205-11.
[18] R. Hashimoto, M. Kanda, H. Takami, D. Shimizu, H. Oya, S. Hibino, Y. Okamura, S. Yamada, T. Fujii, G. Nakayama, H. Sugimoto, M. Koike, S. Nomoto, M. Fujiwara, Y. Kodera, Aberrant expression of melanoma-associated antigen-D2 serves as a prognostic indicator of hepatocellular carcinoma outcome following curative hepatectomy, Oncology letters 9(3) (2015) 1201-1206.
[19] R. Li, J. Gong, C. Xiao, S. Zhu, Z. Hu, J. Liang, X. Li, X. Yan, X. Zhang, D. Li, W. Liu, Y. Chong, Y. Jie, A comprehensive analysis of the MAGE family as prognostic and diagnostic markers for hepatocellular carcinoma, Genomics 112(6) (2020) 5101-5114.
[20] M.J. Yu, R.L. Miller, P. Uawithya, M.M. Rinschen, S. Khositseth, D.W. Braucht, C.L. Chou, T. Pisitkun, R.D. Nelson, M.A. Knepper, Systems-level analysis of cell-specific AQP2 gene expression in renal collecting duct, Proc Natl Acad Sci U S A 106(7) (2009) 2441-6.
[21] M. Bens, V. Vallet, F. Cluzeaud, L. Pascual-Letallec, A. Kahn, M.E. Rafestin-Oblin, B.C. Rossier, A. Vandewalle, Corticosteroid-dependent sodium transport in a novel immortalized mouse collecting duct principal cell line, J Am Soc Nephrol 10(5) (1999) 923-34.
[22] A. Hannemann, J.K. Christie, P.W. Flatman, Functional expression of the Na-K-2Cl cotransporter NKCC2 in mammalian cells fails to confirm the dominant-negative effect of the AF splice variant, J Biol Chem 284(51) (2009) 35348-58.
[23] A. Kompatscher, J.H.F. de Baaij, K. Aboudehen, S. Farahani, L.H.J. van Son, S. Milatz, N. Himmerkus, G.C. Veenstra, R.J.M. Bindels, J.G.J. Hoenderop, Transcription factor HNF1beta regulates expression of the calcium-sensing receptor in the thick ascending limb of the kidney, Am J Physiol Renal Physiol 315(1) (2018) F27-F35.
[24] M.M. Rinschen, M.J. Yu, G. Wang, E.S. Boja, J.D. Hoffert, T. Pisitkun, M.A. Knepper, Quantitative phosphoproteomic analysis reveals vasopressin V2-receptor-dependent signaling pathways in renal collecting duct cells, Proc Natl Acad Sci U S A 107(8) (2010) 3882-7.
[25] S.R.V. Knott, A. Maceli, N. Erard, K. Chang, K. Marran, X. Zhou, A. Gordon, O.E. Demerdash, E. Wagenblast, S. Kim, C. Fellmann, G.J. Hannon, A computational algorithm to predict shRNA potency, Mol Cell 56(6) (2014) 796-807.
[26] C. Kilkenny, W.J. Browne, I.C. Cuthill, M. Emerson, D.G. Altman, Improving bioscience research reporting: the ARRIVE guidelines for reporting animal research, PLoS Biol 8(6) (2010) e1000412.
[27] M.M. Rinschen, X. Wu, T. Konig, T. Pisitkun, H. Hagmann, C. Pahmeyer, T. Lamkemeyer, P. Kohli, N. Schnell, B. Schermer, S. Dryer, B.R. Brooks, P. Beltrao, M. Krueger, P.T. Brinkkoetter, T. Benzing, Phosphoproteomic analysis reveals regulatory mechanisms at the kidney filtration barrier, J Am Soc Nephrol 25(7) (2014) 1509-22.
[28] J. Rappsilber, Y. Ishihama, M. Mann, Stop and go extraction tips for matrix-assisted laser desorption/ionization, nanoelectrospray, and LC/MS sample pretreatment in proteomics, Anal Chem 75(3) (2003) 663-70.
[29] M.P. Bartram, S. Habbig, C. Pahmeyer, M. Hohne, L.T. Weber, H. Thiele, J. Altmuller, N. Kottoor, A. Wenzel, M. Krueger, B. Schermer, T. Benzing, M.M. Rinschen, B.B. Beck, Three-layered proteomic characterization of a novel ACTN4 mutation unravels its pathogenic potential in FSGS, Hum Mol Genet 25(6) (2016) 1152-64.
[30] J.A. Vizcaino, E.W. Deutsch, R. Wang, A. Csordas, F. Reisinger, D. Rios, J.A. Dianes, Z. Sun, T. Farrah, N. Bandeira, P.A. Binz, I. Xenarios, M. Eisenacher, G. Mayer, L. Gatto, A. Campos, R.J. Chalkley, H.J. Kraus, J.P. Albar, S. Martinez-Bartolome, R. Apweiler, G.S. Omenn, L. Martens, A.R. Jones, H. Hermjakob, ProteomeXchange provides globally coordinated proteomics data submission and dissemination, Nat Biotechnol 32(3) (2014) 223-6.
[31] J.A. Vizcaino, A. Csordas, N. del-Toro, J.A. Dianes, J. Griss, I. Lavidas, G. Mayer, Y. Perez-Riverol, F. Reisinger, T. Ternent, Q.W. Xu, R. Wang, H. Hermjakob, 2016 update of the PRIDE database and its related tools, Nucleic Acids Res 44(D1) (2016) D447-56.

[32] J. Cox, M. Mann, MaxQuant enables high peptide identification rates, individualized p.p.b.-range mass accuracies and proteome-wide protein quantification, Nat Biotechnol 26(12) (2008) 1367-72.
[33] S. Tyanova, T. Temu, P. Sinitcyn, A. Carlson, M.Y. Hein, T. Geiger, M. Mann, J. Cox, The Perseus computational platform for comprehensive analysis of (prote)omics data, Nat Methods 13(9) (2016) 731-40.
[34] V.G. Tusher, R. Tibshirani, G. Chu, Significance analysis of microarrays applied to the ionizing radiation response, Proc Natl Acad Sci U S A 98(9) (2001) 5116-21.
[35] N. Colaert, K. Helsens, L. Martens, J. Vandekerckhove, K. Gevaert, Improved visualization of protein consensus sequences by iceLogo, Nat Methods 6(11) (2009) 786-7.
[36] M.E. Ritchie, B. Phipson, D. Wu, Y. Hu, C.W. Law, W. Shi, G.K. Smyth, limma powers differential expression analyses for RNA-sequencing and microarray studies, Nucleic Acids Res 43(7) (2015) e47.
[37] D. Turei, T. Korcsmaros, J. Saez-Rodriguez, OmniPath: guidelines and gateway for literature-curated signaling pathway resources, Nat Methods 13(12) (2016) 966-967.
[38] C.D. Terfve, E.H. Wilkes, P. Casado, P.R. Cutillas, J. Saez-Rodriguez, Large-scale models of signal propagation in human cells derived from discovery phosphoproteomic data, Nat Commun 6 (2015) 8033.
[39] E.L. Huttlin, R.J. Bruckner, J.A. Paulo, J.R. Cannon, L. Ting, K. Baltier, G. Colby, F. Gebreab, M.P. Gygi, H. Parzen, J. Szpyt, S. Tam, G. Zarraga, L. Pontano-Vaites, S. Swarup, A.E. White, D.K. Schweppe, R. Rad, B.K. Erickson, R.A. Obar, K.G. Guruharsha, K. Li, S. Artavanis-Tsakonas, S.P. Gygi, J.W. Harper, Architecture of the human interactome defines protein communities and disease networks, Nature 545(7655) (2017) 505-509.
[40] J. Paek, M. Kalocsay, D.P. Staus, L. Wingler, R. Pascolutti, J.A. Paulo, S.P. Gygi, A.C. Kruse, Multidimensional Tracking of GPCR Signaling via Peroxidase-Catalyzed Proximity Labeling, Cell 169(2) (2017) 338-349 e11.
[41] G.A. Gonzalez, M.R. Montminy, Cyclic AMP stimulates somatostatin gene transcription by phosphorylation of CREB at serine 133, Cell 59(4) (1989) 675-80.
[42] K. Isobe, H.J. Jung, C.R. Yang, J. Claxton, P. Sandoval, M.B. Burg, V. Raghuram, M.A. Knepper, Systems-level identification of PKA-dependent signaling in epithelial cells, Proc Natl Acad Sci U S A 114(42) (2017) E8875-E8884.
[43] K. Yang, X. Huo, Y. Zhang, M. Zhang, Y. Gao, D. Wu, G. Lou, N. Qi, B. Zhang, D. Wang, [Genetic analysis of a pedigree affected with Bartter's syndrome], Zhonghua Yi Xue Yi Chuan Xue Za Zhi 36(7) (2019) 701-703.
[44] J.W. Lee, C.L. Chou, M.A. Knepper, Deep Sequencing in Microdissected Renal Tubules Identifies Nephron Segment-Specific Transcriptomes, J Am Soc Nephrol 26(11) (2015) 2669-77.
[45] M.A. Knepper, Systems biology in physiology: the vasopressin signaling network in kidney, Am J Physiol Cell Physiol 303(11) (2012) C1115-24.
[46] B.L. Allen, D.J. Taatjes, The Mediator complex: a central integrator of transcription, Nat Rev Mol Cell Biol 16(3) (2015) 155-66.
[47] L.K. Schenk, S.J. Bolger, K. Luginbuhl, P.A. Gonzales, M.M. Rinschen, M.J. Yu, J.D. Hoffert, T. Pisitkun, M.A. Knepper, Quantitative proteomics identifies vasopressin-responsive nuclear proteins in collecting duct cells, J Am Soc Nephrol 23(6) (2012) 1008-18.
[48] L. Yu, T. Moriguchi, T. Souma, J. Takai, H. Satoh, N. Morito, J.D. Engel, M. Yamamoto, GATA2 regulates body water homeostasis through maintaining aquaporin 2 expression in renal collecting ducts, Mol Cell Biol 34(11) (2014) 1929-41.
[49] S.T. Lin, C.C. Ma, K.T. Kuo, Y.F. Su, W.L. Wang, T.H. Chan, S.H. Su, S.C. Weng, C.H. Yang, S.L. Lin, M.J. Yu, Transcription Factor Elf3 Modulates Vasopressin-Induced Aquaporin-2 Gene Expression in Kidney Collecting Duct Cells, Front Physiol 10 (2019) 1308.
[50] C.E. Irarrazabal, C.K. Williams, M.A. Ely, M.J. Birrer, A. Garcia-Perez, M.B. Burg, J.D. Ferraris, Activator protein-1 contributes to high NaCl-induced increase in tonicity-responsive enhancer/osmotic response element-binding protein transactivating activity, J Biol Chem 283(5) (2008) 2554-63.

[51] S. Hao, H. Zhao, Z. Darzynkiewicz, S. Battula, N.R. Ferreri, Differential regulation of NFAT5 by NKCC2 isoforms in medullary thick ascending limb (mTAL) cells, Am J Physiol Renal Physiol 300(4) (2011) F966-75.
[52] H.Y. Tseng, L.H. Chen, Y. Ye, K.H. Tay, C.C. Jiang, S.T. Guo, L. Jin, P. Hersey, X.D. Zhang, The melanoma-associated antigen MAGE-D2 suppresses TRAIL receptor 2 and protects against TRAIL-induced apoptosis in human melanoma cells, Carcinogenesis 33(10) (2012) 1871-81.
[53] S. Verma, R. Chanchlani, V.M. Siu, G. Filler, Transient hyponatremia of prematurity caused by mild Bartter syndrome type II: a case report, BMC Pediatr 20(1) (2020) 311.
[54] B.J. Feldman, S.M. Rosenthal, G.A. Vargas, R.G. Fenwick, E.A. Huang, M. Matsuda-Abedini, R.H. Lustig, R.S. Mathias, A.A. Portale, W.L. Miller, S.E. Gitelman, Nephrogenic syndrome of inappropriate antidiuresis, The New England journal of medicine 352(18) (2005) 1884-90.
[55] K. Xiao, J. Sun, J. Kim, S. Rajagopal, B. Zhai, J. Villen, W. Haas, J.J. Kovacs, A.K. Shukla, M.R. Hara, M. Hernandez, A. Lachmann, S. Zhao, Y. Lin, Y. Cheng, K. Mizuno, A. Ma'ayan, S.P. Gygi, R.J. Lefkowitz, Global phosphorylation analysis of beta-arrestin-mediated signaling downstream of a seven transmembrane receptor (7TMR), Proc Natl Acad Sci U S A 107(34) (2010) 15299-304.
[56] A.R.B. Thomsen, B. Plouffe, T.J. Cahill, 3rd, A.K. Shukla, J.T. Tarrasch, A.M. Dosey, A.W. Kahsai, R.T. Strachan, B. Pani, J.P. Mahoney, L. Huang, B. Breton, F.M. Heydenreich, R.K. Sunahara, G. Skiniotis, M. Bouvier, R.J. Lefkowitz, GPCR-G Protein-beta-Arrestin Super-Complex Mediates Sustained G Protein Signaling, Cell 166(4) (2016) 907-919.
[57] A. Datta, C.R. Yang, K. Limbutara, C.L. Chou, M.M. Rinschen, V. Raghuram, M.A. Knepper, PKA-independent vasopressin signaling in renal collecting duct, FASEB J 34(5) (2020) 6129-6146.

Figure 1. MAGED2 is expressed in the distal part of the mouse nephron in early embryonic stages. (A) qPCR analysis of Maged2 mRNA expression in murine embryonal tissue at the indicated embryonic stages. P<0.05 in one-way ANOVA followed by Tukey's post test for E14. vs newborn. (B) qPCR analyses of the mRNA expression of the crucial transporters NCC, NKCC2 and AQP2 of murine embryonic tissue at the indicated embryonic stages. *P<0.05 in one-way ANOVA followed by Tukey's post test.

Figure 2. MAGED2 is a putative regulator of G-protein coupled receptor signalling. (A) Western Blot analysis of MAGED2 in HEK293T cells treated with either scrambled (scr) control siRNA or MAGED2 siRNA. Beta Actin is used as loading control. (B) Proteome analysis of HEK293T cells after treatment with MAGED2 siRNA in comparison to scrambled siRNA treated control cells. Each dot represents a protein. Only the expression of MAGED2 was significantly altered (FDR = 0.05).
(C) Phosphoproteome analysis of the same HEK293T cells as in B after treatment with MAGED2 siRNA in comparison to control cells. Each dot represents a phosphorylation site. Known PKA phosphorylation are labelled with their gene symbol. (D) Characterization of the altered phosphorylation motifs by classifying motifs as basophilic or not (based on presence of R or K at the -3 position). Here was an overrepresentation of basophilic motifs in the phosphorylation sites decreased by MAGED2 knockdown. Fisher's exact test p<0.001. (E) Sequence logos showing overrepresented phosphorylation motifs increased and decreased in HEK293T cells after MAGED2 siRNA treatment. (F) Scatterplot indicating MAGED2 siRNA-induced changes in phosphoproteome (y axis) and proteome (x-axis) in HEK293T cells. Phosphorylation sites are more strongly affected by MAGED2 siRNA. (G) Reanalysis of published proteins in proximity to AT1R-APEX after angiotensin II treatment at two different time points [40]. MAGED2 is recruited to AT1R after 21 minutes.

Figure 3: MAGED2 modulates short-term V2R dependent signalling in mpkCCD cells.
(A) RT-qPCR analysis of MAGED2 mRNA expression in MAGED2 hp and control cells.
(B) Western Blot analysis of MAGED2 protein abundance in mpkCCD MAGED2 hp and control cells. Actin served as loading control. (C) Time course of cAMP levels in mpkCCD cells after 1 nM dDAVP treatment at the indicated time points. *p<0.05 in a two-tailed t-test, n=3 (hairpins) or 4 (control). (D) Western Blot analysis of pCREB in mpkCCD cells after short-term treatment with 1 nM dDAVP for 30 minutes. The short-term exposure was preceded by a long-term exposure followed by a 6h dDAVP starvation. For the quantification, the pCREB level was normalized with the corresponding total CREB level signal and the logarithmic ratio of dDAVP treated to untreated sample was plotted (n=5; *P < 0.05, in a paired two-tailed t-test). (E) Western Blot analysis of pERK in mpkCCD cells after short-term treatment with 1 nM dDAVP for 30 minutes. The short-term exposure was preceded by a long-term exposure followed by a 6h dDAVP starvation. For the quantification, the pERK level was normalized with the corresponding total ERK level signal and the logarithmic ratio of dDAVP treated to untreated sample was plotted (n=5; one‑way ANOVA, Dunnett's multiple comparison test). (F)

Scatterplot of phosphorylation sites perturbed by dDAVP in MAGED2 hp versus control cell lines. Density is coded by colour. Overall, a moderate correlation of vasopressin induced phosphorylation in hp and control cells is observed (R=0.25). Black: known PKA phosphorylation sites. (G) Sequence logos showing overrepresented phosphorylation motifs increased and decreased in MAGED2 hp and control mpkCCD cells after short-term dDAVP treatment. (H) Characterization of the increased phosphorylation motifs by classifying motifs as basophilic or not (based on presence of R or K at the -3 position). Fraction of basophilic sites was reduced in MAGED2 hp cells (p=0.03 in Chi-Square test).

Figure 4: MAGED2 modulates long-term V2R dependent signalling in mpkCCD cells. (A) Proteome analysis of mpkCCD hp and control cells after long-term (72h) dDAVP treatment. Each dot represents a protein and its ratio of ddAVP/vehicle in the respective cell lines. Aquaporin-2 and Med14 were significantly increased in MAGED2 hp cells after dDAVP treatment (n=3 replicates). (B) AQP2 mRNA expression in mpkCCD cells after 72 hours of dDAVP treatment (n=3; **P<0.01; ***P<0.001; one‑way ANOVA, Dunnett's multiple comparison test). (C) Western Blot analysis of AQP2 protein in mpkCCD cells after 72 hours of dDAVP treatment. (n=3; ****P<0.0001; one‑way ANOVA, Dunnett's multiple comparison test).

Figure S1. qPCR analysis of MAGED2 protein in murine embryonal tissue at the indicated embryonic stages and discriminated between male and female.

Figure S2. Analysis of the phosphoproteomic data concerning differences in the phosphorylation networks between control and hp cells obtained from PHONEMeS[38]. The red-bordered square nodes represent significantly perturbed phospho-sites. Green-filled and yellow-filled nodes both represent proteins that are found in both networks, whereas the yellow-filled nodes have different phosphorylation sites. Considerable network rewiring can be observed.

Figure S3. Western Blot analysis of pAQP2 in mpkCCD cells after short-term treatment with 1 nM dDAVP for 30 minutes. A long-term treatment of 72 hours and a subsequent starvation without dDAVP for 6 hours preceded this procedure to gain sufficient protein levels of total AQP2. For the quantification the pAQP2 signals were normalized with their corresponding unphosphorylated signal and illustrated as a scatter plot of the mean of the logarithmic relation of treated sample to untreated sample and the SD (N=4; one‑way ANOVA, Dunnett's multiple comparison test).

Figure S4. *Scnn1b* mRNA expression in mpkCCD cells after 72 hours of dDAVP treatment (n=3; one‑way ANOVA, Dunnett's multiple comparison test).

Figure S5. *Avpr2* mRNA expression in mpkCCD cells after 72 hours of dDAVP treatment (n=3; one‑way ANOVA, Dunnett's multiple comparison test).

Supplemental Table 1. Proteomic analysis of MAGED2 knockdown cells.
Supplemental Table 2. Phosphoproteomic analysis of MAGED2 knockdown cells.
Supplemental Table 3. Phosphoproteomic analysis of MAGED2 knockdown mpkCCD cells in the presence of short-term vasopressin exposure.
Supplemental Table 4. Proteomic analysis of MAGED2 knockdown mpkCCD cells in the presence of long-term (72h) vasopressin exposure.

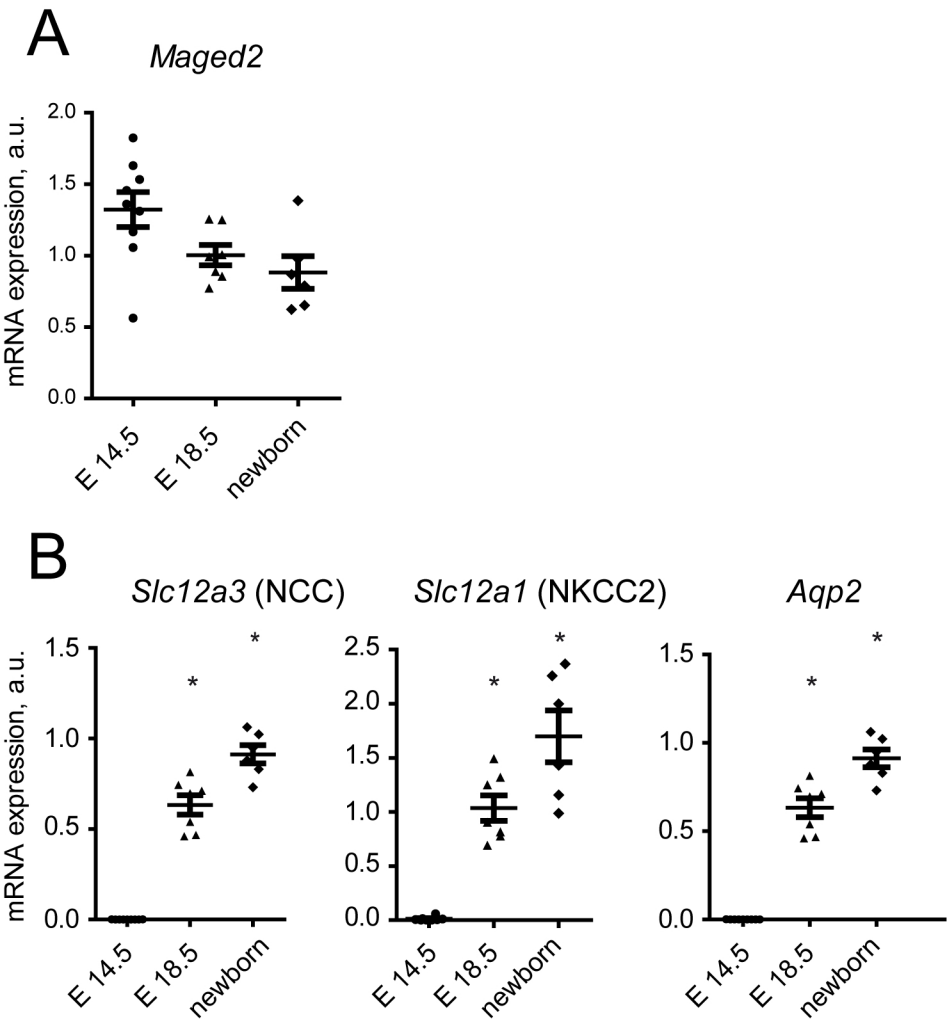
A
Maged2
mRNA expression, a.u.
2.0
1.5
1.0
0.5
0.0
E 14.5
E 18.5
newborn
B
Slc12a3 (NCC)
Slc12a1 (NKCC2)
Aqp2
mRNA expression, a.u.
1.5
1.0
0.5
0.0
2.5
2.0
1.5
1.0
0.5
0.0
*
E 14.5
E 18.5
newborn

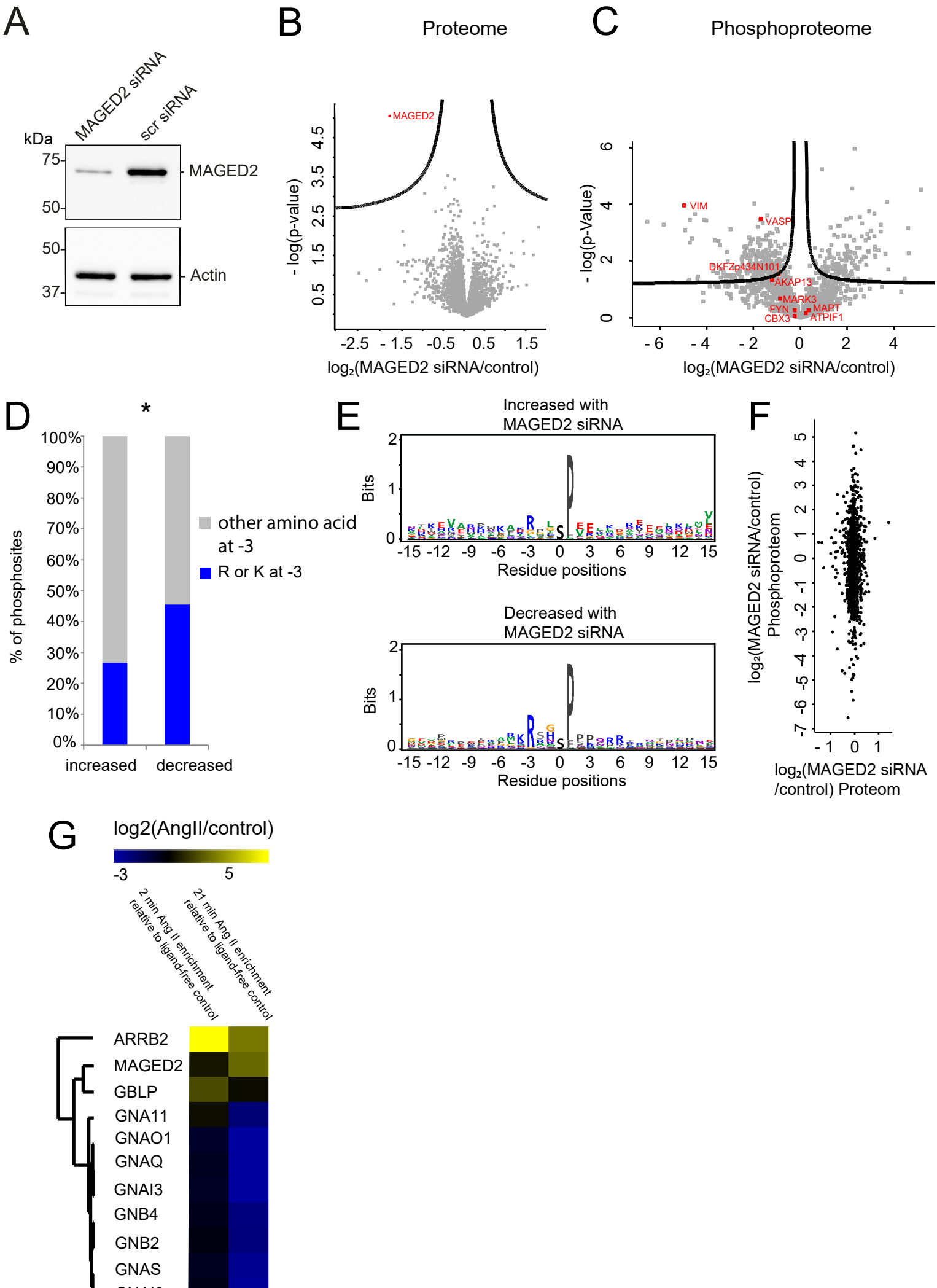
A
MAGED2 siRNA
scr siRNA
kDa
75
50
MAGED2
50
37
Actin
B
Proteome
MAGED2
- log(p-value)
log2(MAGED2 siRNA/control)
C
Phosphoproteome
VIM
VASP
DKFZp434N101
AKAP13
MARK3
FYN
CBX3
MAPT
ATPIF1
- log(p-Value)
log2(MAGED2 siRNA/control)
D
*
% of phosphosites
other amino acid at -3
R or K at -3
increased
decreased
E
Increased with MAGED2 siRNA
Bits
Residue positions
Decreased with MAGED2 siRNA
F
log2(MAGED2 siRNA/control) Phosphoproteom
log2(MAGED2 siRNA /control) Proteom
G
log2(AngII/control)
-3
5
2 min Ang II enrichment relative to ligand-free control
21 min Ang II enrichment relative to ligand-free control
ARRB2
MAGED2
GBLP
GNA11
GNAO1
GNAQ
GNAI3
GNB4
GNB2
GNAS
GNAI2

Fig. 2

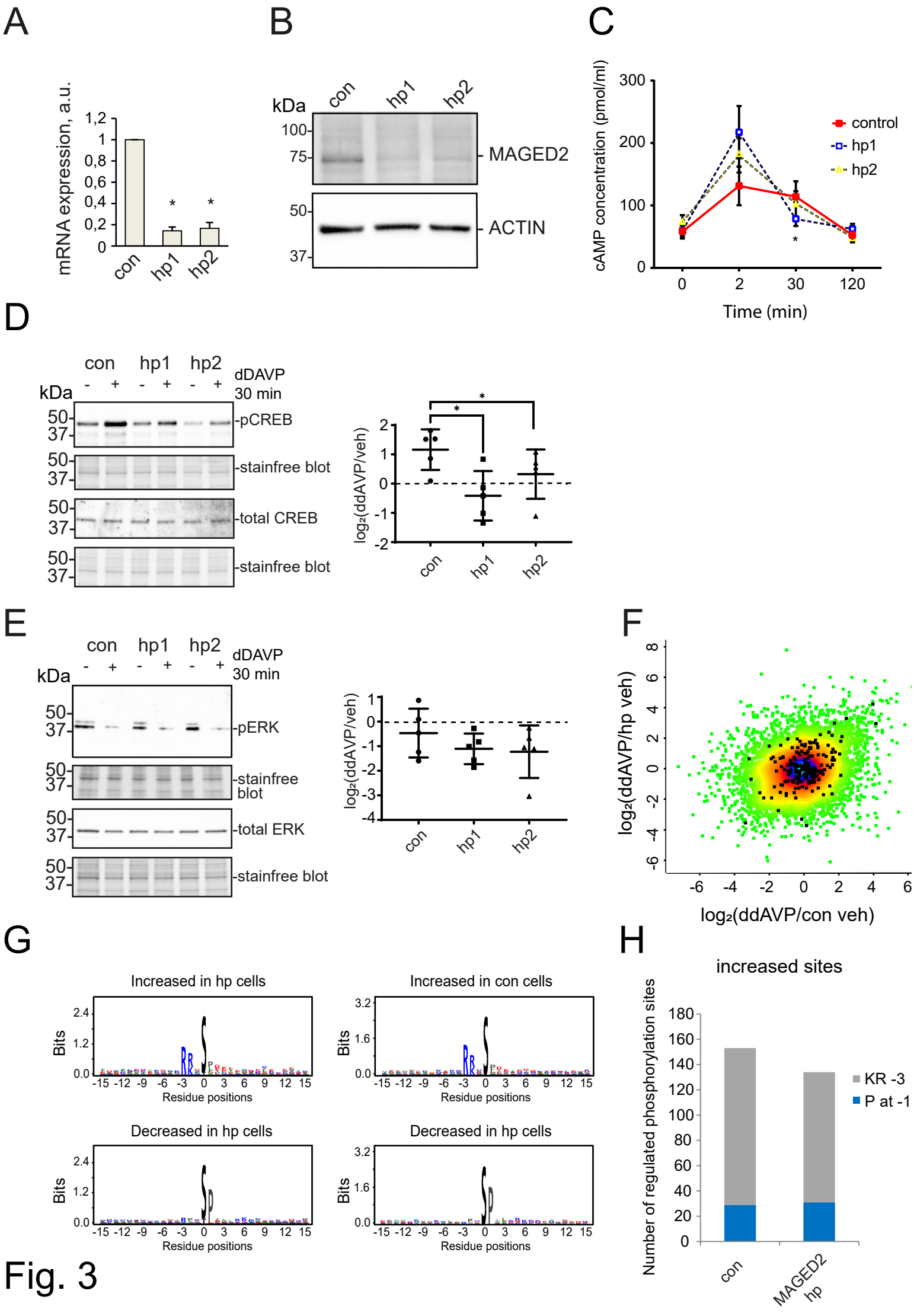
A
mRNA expression, a.u.
1,2
1
0,8
0,6
0,4
0,2
0
con
hp1
hp2
B
kDa
con
hp1
hp2
100
75
MAGED2
50
ACTIN
37
C
cAMP concentration (pmol/ml)
300
200
100
0
control
hp1
hp2
0
2
30
120
Time (min)
D
con
hp1
hp2
dDAVP
30 min
kDa
pCREB
stainfree blot
total CREB
stainfree blot
log2(ddAVP/veh)
E
con
hp1
hp2
dDAVP
30 min
kDa
pERK
stainfree blot
total ERK
stainfree blot
log2(ddAVP/veh)
F
log2(ddAVP/hp veh)
log2(ddAVP/con veh)
G
Increased in hp cells
Increased in con cells
Decreased in hp cells
Decreased in hp cells
Bits
Residue positions
H
increased sites
Number of regulated phosphorylation sites
KR -3
P at -1
con
MAGED2 hp

Fig. 3

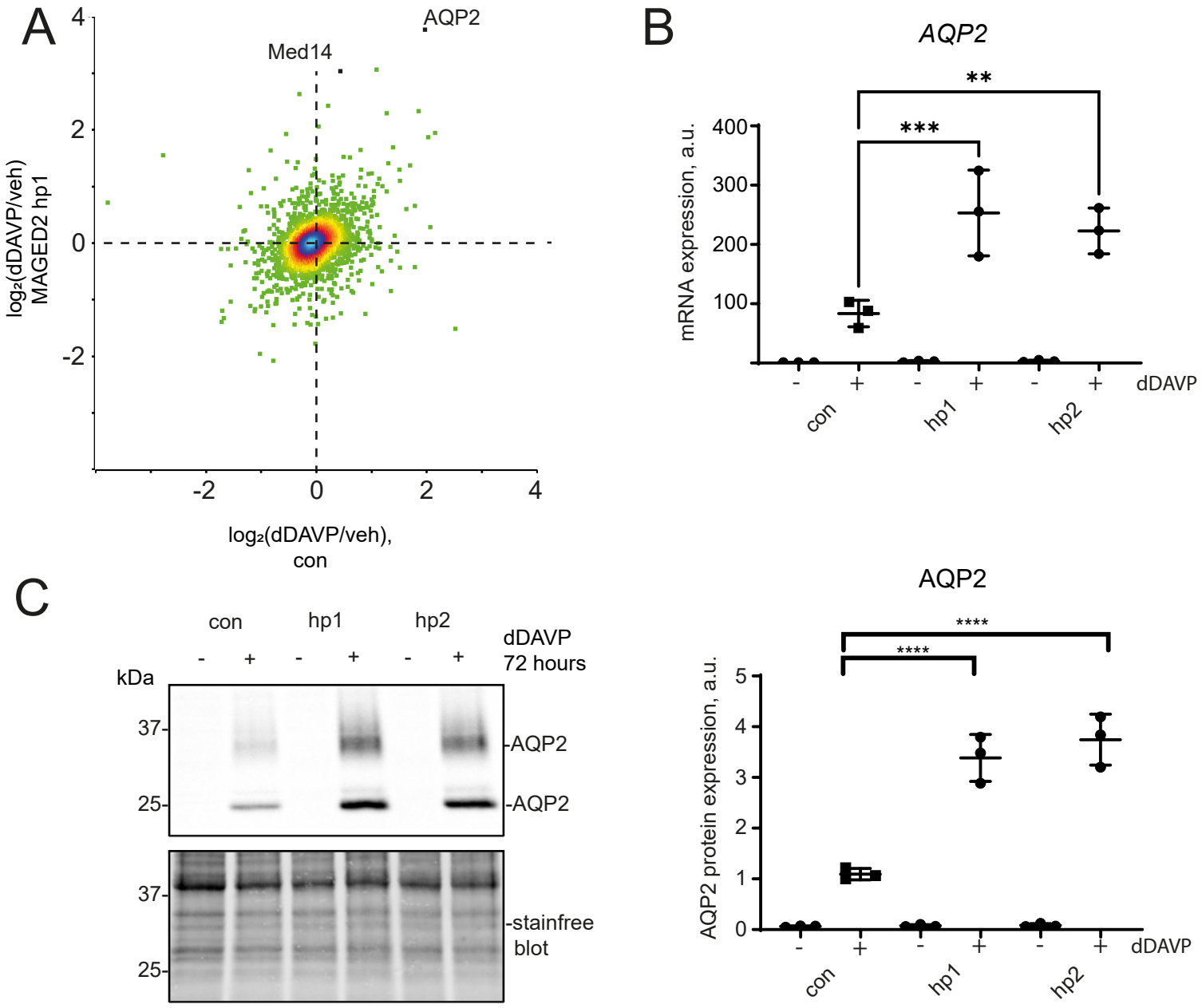
A
AQP2
Med14
log₂(dDAVP/veh)
MAGED2 hp1
log₂(dDAVP/veh),
con
B
AQP2
mRNA expression, a.u.
dDAVP
con
hp1
hp2
C
con
hp1
hp2
dDAVP
72 hours
kDa
-AQP2
-AQP2
-stainfree
blot
AQP2
AQP2 protein expression, a.u.

Fig. 4